2025 International Conference on Mobile and Miniaturized Terahertz Systems (ICMMTS) | 979-8-3503-6583-2/25/$31.00 ©2025 IEEE | DOI: 10.1109/ICMMTS62835.2025.10925984

How to Build a Multi-Kilometer Terabit-Per-Second Sub-Terahertz Wireless Backhaul

Duschia Bodet
Department of Electrical and Computer Engineering
Northeastern Univeristy
Boston, USA
bodet.d@northeastern.edu

Josep M. Jornet
Department of Electrical and Computer Engineering
Northeastern Univeristy
Boston, USA
j.jornet@northeastern.edu

***Abstract*—Over the past several decades the terahertz - and more specifically the sub-terahertz (sub-THz) - band has been explored as an enabling technology for future wireless communications systems. However, there has yet to be a practical system architecture to actualize long-range, terabit-per-second (Tbps), links. In this paper, a potential system design for a multi-kilometer, Tbps wireless backhaul using sub-THz communications is provided. The presented system implements an array of subarrays or an array of directional antennas architecture to perform distributed multiple-input multiple-output (MIMO), and the analytical results demonstrate the potential of the system to support Tbps links over multiple kilometers.**

***Index Terms*—Sub-THz communications, Tbps, wireless backhaul**

I. Introduction

Over the past several decades the terahertz - and more specifically sub-terahertz (sub-THz) - band has been explored as an enabler for future wireless communications. Loosely defined to span from 100 to 500 GHz, the sub-THz band has broad available chunks of spectrum that can support terabit-per-second (Tbps) wireless links. If such links could provide low-latency and long-range communications, they would make a viable alternative to the expensive fiber optics infrastructure and could one day be a part of bridging the digital divide.

However, there has yet to be a practical system architecture to actualize Tbps links, and this implementation is still an open research question. With the exception of a few works [1], [2], much of the recent focus for sub-THz communications has been on short-range applications. This focus is understandable given the notoriously low transmission power of sub-THz devices, and the fact that much of the technology is still emerging. But, if we hope to use sub-THz to bridge the digital divide, long-range high-capacity links are necessary, and in this paper, we will show that they are closer to a reality than one might expect.

The rest of this paper is organized as follows: Sec. II explains the reasoning behind the chosen system model, and then the model is described in Sec. III. We also provide the necessary derivations given physical and practical constraints and present the numerical results along with discussions in Sec. IV. In Sec. V we provide some thoughts on what parts of the research must still be done for multi-kilometer Tbps links to become a reality, before offering concluding remarks in Sec. VI.

This work was supported by NSF CNS-1955004.

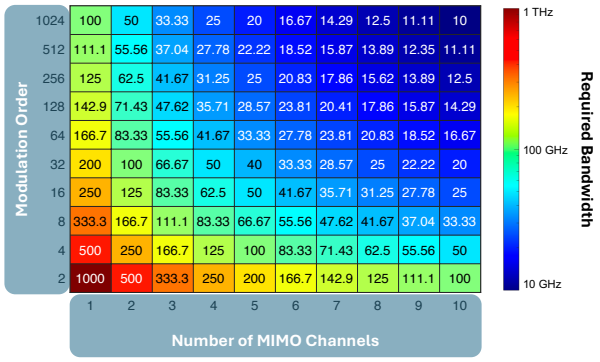

Fig. 1. Amount of bandwidth required to achieve a Tbps link with a given modulation order and number of MIMO channels

II. Motivation for the Chosen System Model

To perform this analysis, we start with our objective in mind: a multi-kilometer, Tbps link.

A. MIMO Channels are Necessary

It has been shown in [3] that in addition the broad bandwidths available at sub-THz frequencies, multiple-input multiple-output (MIMO) channels will also be required to reach Tbps links. In Fig. 1 we show in a color gradient the bandwidth required to reach a Tbps link with a certain modulation and a certain number of MIMO channels as dictated by

$$1 * 10^{12} = BW * \log_2(M)\, N_{MIMO}, \tag{1}$$

where BW is the bandwidth, M is the modulation order, and N_{MIMO} is the number of MIMO channels. Although, theoretically, one could try to design a system with one MIMO channel using 100 GHz centered perhaps at 500 GHz, using such a broad bandwidth is impractical both from a hardware perspective and a spectrum sharing/allocation perspective. In other words, it is difficult to both build devices with relatively steady performance across 50 GHz of bandwidth and to obtain

licensing to legally use that much bandwidth. Especially considering many sensitive passive devices, the available spectrum within the sub-THz band is not all contiguous. Thus, MIMO channels are necessary to build our practical multi-kilometer Tbps link.

B. Achieving MIMO Channels in LoS Scenarios

It has also been thoroughly demonstrated that the sub-THz MIMO channel is primarily line-of-sight (LoS) [4]. Particularly for the case of a multi-kilometer link, given the high propagation loss of sub-THz signals, combined with the required directivity of the transmissions to overcome this path loss, we will not be able to rely on multi-path propagation to provide a spatial multiplexing gain as is often done at lower frequencies. Many recent works have explored methods for achieving spatial multiplexing in sub-THz LoS MIMO. Chief among the strategies presented are:

1) using the near-field propagation characteristics to carefullly space the antenna elements in a way that maximizes the channel gains [5]–[7]
2) using different polarizations [8] or different levels of orbital angular momentum (OAM) [9] to create orthogonal channels
3) using the antenna element directionality to create orthogonal channels in an array of sub-arrays (AoSA) or array of directional antennas (AoDA) architecture [10], [11]

One could argue that the third strategy is a special case of the first. Again, keeping our objective of a Tbps multi-kilometer wireless backhaul in mind, we start our analysis following Option 3, and later provide discussion on potentially extending to include different polarizations. We refrain from starting with Option 2 because although polarization multiplexing can successfully and simply increase the system capacity by a factor of two or three, using polarization as the primary multiplexing technology limits the number of possible MIMO channels to the number of possible polarizations. As for OAM channels, the divergence of the OAM beams often necessitates that either the transmitter and receiver are large with close to full phase and amplitude control over the entire aperture to successfully (de)multiplex multiple OAM modes (a computationally expensive and difficult-to-fabricate architecture), or that the transmitter's antenna aperture or uniform circular array (UCA) be smaller than the receiver's [12]. This asymmetry is not ideal for wireless backhaul systems that would need full-duplex capabilities. Although there has been work showing potential strategies to mitigate the divergence [12], [13] that could lead to OAM being a viable future solution for some applications, Option 3 provides simpler implementation and we continue with this strategy to design our system.

III. System Model

We use the system model shown in Fig. 2 as a starting point, where each green square represents a single subarray or directional antenna element with dimension D_{sub}. We emphasize that this architecture is possible with either the AoSA or AoDA architecture. For this analysis and generality, we consider on the AoSA architecture for this analysis and at the end offer some discussion about the possibilities for the AoDA architecture.

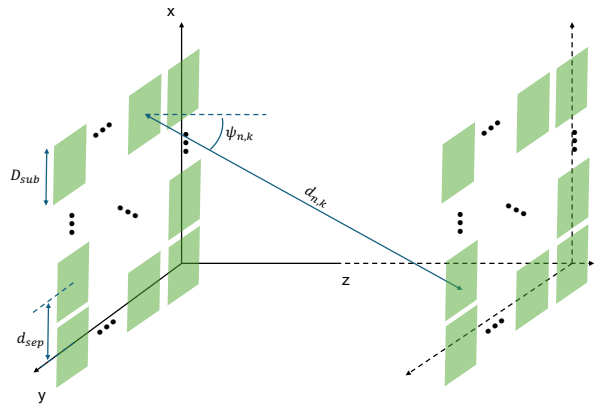

Fig. 2. System model for an arbitrary number of subarrays.

The separation between subarrays is given by d_{sep}, and the transmission distance between the *n*th transmit antenna and the *k*th receive antenna is given by $d_{n,k}$, with $\psi_{n,k}$ representing the angle between $d_{n,k}$ and the normal. For symmetry, we consider identical transmit and receive architectures and that each subarray is steered to its normal. The length and width of each AoSAs is given by $d_{sep}(N_{x/y}-1)+D_{sub}$, where

$$N_x = \frac{N_{subarrays}}{\lfloor\sqrt{N_{subarrays}}\rfloor}, \tag{2}$$

and

$$N_y = \lfloor\sqrt{N_{subarrays}}\rfloor. \tag{3}$$

We begin by determining several practical restrictions for the system given the required transmission distance and the chosen architecture.

First, although strategy 1 for generating LoS MIMO channels, relies on the entire transmit and receive antenna arrays being in each others' near field such that the phase difference in paths between pairs of transmitting and receiving antennas is distinguishable [14], in order to accurately calculate the propagation characteristics for each sub-channel, each subarray will need to be operating in its far-field region. Aside from the untraditional propagation loss that occurs in the near-field that has only begun to be characterized, if we plan to utilize the antenna elements' or subarrays' directivity to improve the design performance, it is important to note that their directivity can be substantially reduced within their near-field region [15]. Therefore, we should be in the far-field of these elements/subarrays so that the directivity and propagation losses observed from each subarray are as anticipated. Thus according to the Fraunhofer equation [16],

$$D_{sub} \leq \frac{\sqrt{z\max(\lambda)}}{4}, \tag{4}$$

where z is the transmission distance, and $\max(\lambda)$ is the largest wavelength used in the broadband signal. Theoretically, d_{sep}

could be as small as D_{sub}, however, different separations will have different performances [6], [10], so in our analysis, we will sweep $D_{sub} \leq d_{sep} \leq z\tan(\theta_{3dB})$, where θ_{3dB} is the 3 dB beamwidth of the subarrays and can be found using knowledge of the subarray size to find the minimum gain [14] $G_{min} = \frac{4\pi D_{sub}^2}{\max(\lambda)^2}$ (i.e. the gain corresponding to the maximum wavelength and the largest 3dB-beamwidth, which we find according to

$$\theta_{3dB} = 2\arccos\left(1 - \frac{2}{G_{min}}\right). \tag{5}$$

The channel matrix for this system is given by

$$H = \begin{bmatrix} h_{1,1} & ... & h_{n,1} & ... & h_{N_{tx},1} \\ h_{1,2} & ... & h_{n,2} & ... & h_{N_{tx},1} \\ . & . & & . & . \\ . & . & & . & . \\ . & . & & . & . \\ h_{1,N_{rx}-1} & ... & h_{n,N_{rx}-1} & ... & h_{N_{tx},N_{rx}-1} \\ h_{1,N_{rx}} & ... & h_{n,N_{rx}} & ... & h_{N_{tx},N_{rx}} \end{bmatrix}, \tag{6}$$

where $h_{n,k}$ is a vector representing the channel between the nth transmit and kth receive subarray. We find $h_{n,k}$ according the frequency-dependent path and absorption loss, propagation phase, and subarray radiation pattern, $\beta_{n,k}(\psi_{n,k}, f)$, like so:

$$h_{n,k} = \alpha_{n,k}\left(d_{n,k}, f\right)\beta_{n,k}(\psi_{n,k}, f)\beta_{n,k}(\psi_{n,k}, f)e^{j2\pi d_{n,k}/\lambda}. \tag{7}$$

Where we have taken $\alpha_{n,k}\left(d_{n,k}, f\right)$ to be the combined spreading and absorption loss and $\beta_{n,k}(\psi_{n,k}, f)$ to be the radiation pattern of a square phased array of patch antennas spaced $\lambda_c/2$ and with height and width of $\lambda_c/4$, λ_c is the center wavelength. We find $\beta_{n,k}(\psi_{n,k}, f)$ according to to [16], and leave the expression out for brevity. From H, we can calculate the channel rank and condition number to determine the feasibility of spatial multiplexing. To estimate the transmission power required to close the link, we determine a target signal-to-noise ratio (SNR) threshold and perform the following calculation:

$$P_{TX} = \sum_{f_c - \frac{BW}{2}}^{f_c + \frac{BW}{2}} \frac{SNR_{req} k_B T \Delta f}{G^2(f) L(f)}, \tag{8}$$

where SNR_{req} is the SNR threshold, k_B is the Boltzmann constant, T is room temperature in Kelvin, and $G(f)$ and $L(f)$ are the frequency-dependent subarray gain and path loss respectively.

IV. Results

We now present analytical results indicating the performance of a system with the architecture described in Sec. III.

A. Condition Number

In Fig. 3, we show the results for a system with 4 subarrays, aiming to use 4 MIMO channels, each with 25 GHz of bandwidth. From Fig. 1, we recall that such a system would have to use a modulation order of 1024 to reach Tbps speeds. We start by calculating the condition number for three possible center frequencies within the sub-THz band (150 GHz, 350 GHz, and 500 GHz) for five potential transmission distances (from 1 to 5 km) as a function of frequency and the subarray separation. Although the channel rank is a common metric to determine the number of linearly independent rows or columns, which indicates the number of independent subchannels that exist, the condition number provides a clearer picture of how well those subchannels can feasibly support spatial multiplexing [17]. In practice condition numbers below 10 dB are very good, and condition numbers above 20 dB indicate that it is virtually impossible to do spatial multiplexing. Thus, for ease of comparison and without compromising the practical implications of the results, we have limited our color scale in Fig. 3 to 20 dB, and any larger condition numbers are clipped. The x-axis of each plot is the range of frequencies occupied by the 25 GHz bandwidth, and the y-axis is the subarray separation in meters. Each row in the subfigure corresponds to a certain center frequency, while each column corresponds to a certain transmission distance.

Keeping with the findings of previous works [6], [10], the channel's ability to support spatial multiplexing varies periodically with the subarray separation. We see this especially with small separations, and this periodicity (i.e. the blue and yellow horizontal lines) diminishes as the antenna separation increases and/or as the transmission distance decreases. This trend is due to the antenna elements' directivity playing a more dominant role as the subarrays are moved farther apart and/or as the transmitter and receiver are brought closer together.

We also notice that the frequency dependence means that at some subarray separations, the condition number is not constant across the entire signal bandwidth. This is especially noticeable in the lower frequency range with the 140 GHz center frequency; the bright horizontal lines are slanted. For a system to support spatial multiplexing across the entire 25 GHz of bandwidth, we are essentially looking for a horizontal line within these plots that remains in the dark blue or green region. There are obviously many options when the array separation is large (greater than 8 m, 5 m, and 4 m for 5 km links at 150 GHz, 350 GHz, and 500 GHz, respectively), but for ease of fabrication and deployment, it is generally preferred to have smaller systems. From Fig. 3, we see that there are indeed smaller subarray separations that can support multiplexing links. For example, in Fig. 3m, for a 3 km link centered at 500 GHz, the subarrays can be separated a little less than 1 m with $D_{sub} \approx 34\ cm$. For the 4x4 MIMO system considered in this case, that would mean the full aperture size would be smaller than 1.5 m x 1.5 m, which is a practical size for deployment.

B. Required Transmission Power

Aside from determining whether spatial multiplexing is feasible in the given scenario, it is also important that the transmission power required to achieve Tbps speeds is within reason.

To evaluate this, we first determine the required SNR for reasonable performance. According to Fig. 1, a 4-channel system with 25 GHz of bandwidth would need to support

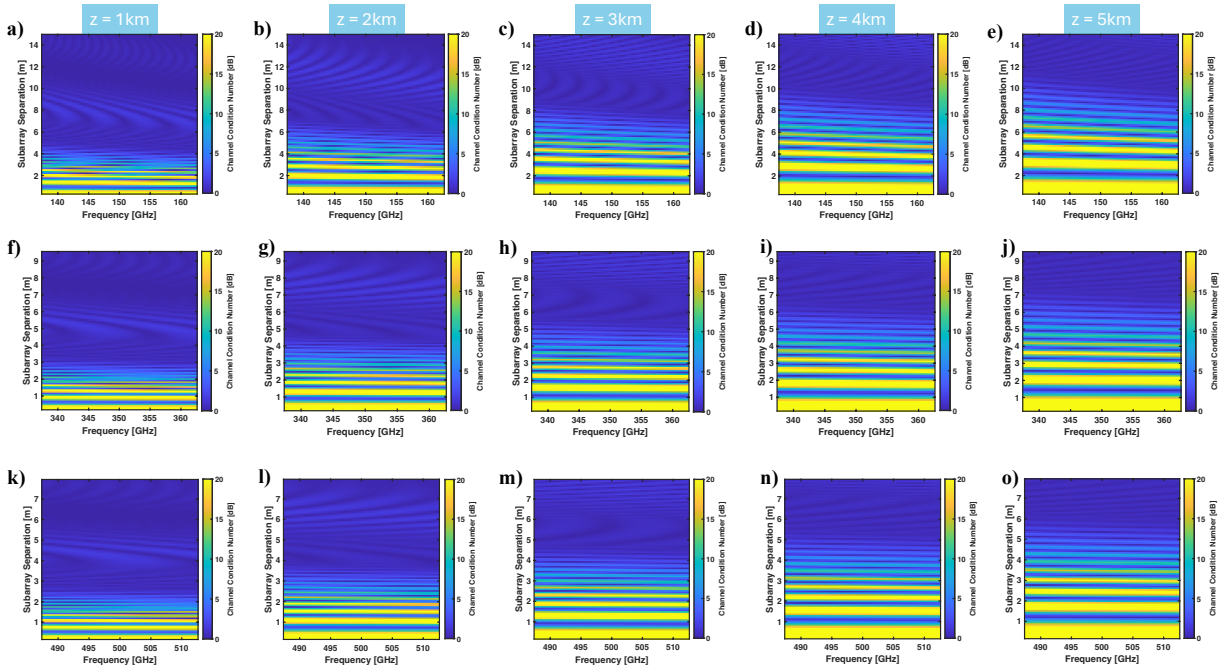

Fig. 3. Channel Condition Number over the operational bandwidth of the system for different subarray separations for a 150 GHz system with transmission distances of (a) 1 km, (b) 2 km, (c) 3 km, (d) 4 km, (e) 5 km; for a 350 GHz system with transmission distances of (a) 1 km, (b) 2 km, (c) 3 km, (d) 4 km, (e) 5 km; and a 500 GHz system with transmission distances of (a) 1 km, (b) 2 km, (c) 3 km, (d) 4 km, (e) 5 km.

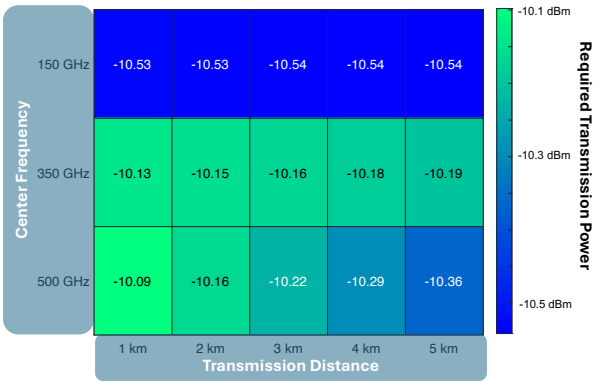

Fig. 4. Total Transmission Power Required to Support a Tbps link using 4 MIMO channels

a modulation order of 1024 in order to reach Tbps speeds. Recalling that the probability of error for an M-QAM system is given by [18]:

$$P_{err} = 4\left(1 - \frac{1}{\sqrt{M}}\right) Q\left(\sqrt{\frac{3\log_2(M) SNR \frac{BW}{f_b}}{M-1}}\right), \quad (9)$$

where f_b is the bit rate. We can plot the error rate as a function of SNR (excluded in this paper for brevity) and determine that to achieve an error rate of 10^{-6}, the SNR should be close to 30 dB. Equation (8) demonstrates how we can use this threshold to calculate the required power and results for the same 4x4 MIMO system described previously are shown in Fig. 4. Although these values may seem uncharacteristically low for multi-kilometer, Tbps links recall that the high gain of the subarrays significantly reduces the required transmit power making these systems relatively efficient.

One other point of consideration in terms of the transmit power is that although the required SNR will be the same for different implementations of a 1024-QAM (i.e., single-carrier, orthogonal frequency division multiplication (OFDM), and discrete Fourier transform spread OFDM (DFT-spread OFDM)), the average power for each implementation will be slightly different considering the peak-to-average-power ratio (PAPR). A single-carrier system with frequency-domain pre and post-equalization would likely offer the best performance in terms of transmission power efficiency, but processing power should also be considered to optimize the system performance. The results in Fig. 4 offer a general approximation of the required transmission power that should be expected.

V. Future Directions

In this paper we have shown a physical implementation that would allow for multi-kilometer Tbps links. The design is fairly straightforward, and can likely lend itself to implementation in the near future. There are, however, a few areas of research that must be addressed in order for these links to become a reality. In this section, we discuss what those areas are, and how we might adapt the system model accordingly.

A. Optimizing for Bandwidth and Power Limitations of the Hardware Back-end

Perhaps one of the largest remaining challenges in creating broadband sub-THz systems is creating a digital back-end capable of processing incoming data at Tbps speeds.

Although there have been some works demonstrating real-time processing for sub-THz communications, to the authors' knowledge 48 Gbps is the highest speed shown to be processed in real-time over a total bandwidth of 8 GHz [19]. Aside from improving the capabilities of real-time processing platforms, this challenge can also be addressed by reducing the amount of bandwidth used by the backhaul system or conversely increasing the number of MIMO channels. These additional channels could be added as spatially multiplexed channels as shown above or as a combination of spatially multiplexed and polarization multiplexed channels to relax some of the design constraints.

On the other hand, although the required radio frequency power is low, the true power drain will come from the hardware back-end, particularly the analog-to-digital converters (ADCs) and digital-to-analog converters (DACs) on each RF chain. From this perspective, fewer MIMO channels would be preferred. Thus, there will need to be some compromise and optimization to find the appropriate number of MIMO channels and modulation order to allow for realistic bandwidth and power consumption given the hardware back-end.

B. Finding the Ideal Subarray or Directional Element

Another fabrication challenge and expense would be creating subarrays large enough for the proposed architecture if traditional phased arrays are considered. Fortunately, for this backhaul application, the system would likely be static, and therefore these subarrays would likely not need to be steered individually, which would eliminate the requirement for adjustable phase shifters at each element. Still, to the authors' knowledge, the current largest phased array at sub-THz frequencies has 128 active elements [20], and for the presented analysis, we would need subarrays with up to 300 elements. One potential solution would be to use directional antenna elements such as horn or dish antennas instead of subarrays. This approach would also help ensure that the signals being combined by each element of the phased array are more than just noise. However, future analysis should consider more thoroughly when and whether steering would be required. An important question is how resilient such a system would be to slight misalignments and the architecture may need to be adapted for a case where steering is required (i.e., in a non-terrestrial network, for example).

VI. Conclusion

In this paper, we answer the practical question of designing a multi-kilometer Tbps wireless backhaul using sub-THz communications. The presented system uses an AoSA or AoDA architecture to perform distributed MIMO, and analytical results demonstrate the system's potential to support Tbps links over multiple kilometers. Future directions to make such a system a reality are also discussed, and we look forward to seeing high-speed sub-THz backhauls be part of the solution to today's digital divide.

References

[1] J. Ding, J. Yu, W. Li, K. Wang, W. Zhou, J. Zhang, M. Zhu, T. Xie, J. Yu, and F. Zhao, "High-speed and long-distance photonics-aided terahertz wireless communication," *Journal of Lightwave Technology*, vol. 41, no. 11, pp. 3417–3423, 2023.

[2] P. Sen, J. V. Siles, N. Thawdar, and J. M. Jornet, "Multi-kilometre and multi-gigabit-per-second sub-terahertz communications for wireless backhaul applications," *Nature Electronics*, vol. 6, no. 2, pp. 164–175, 2023.

[3] M. Polese, X. Cantos-Roman, A. Singh, M. J. Marcus, T. J. Maccarone, T. Melodia, and J. M. Jornet, "Coexistence and spectrum sharing above 100 ghz," *Proceedings of the IEEE*, 2023.

[4] D. Bodet, P. Dinh, M. Stojanovic, J. Widmer, D. Koutsonikolas, and J. M. Jornet, "Characterizing sub-thz mimo channels in practice: a novel channel sounder with absolute time reference," in *GLOBECOM 2023-2023 IEEE Global Communications Conference*. IEEE, 2023, pp. 1459–1464.

[5] H. Do, S. Cho, J. Park, H.-J. Song, N. Lee, and A. Lozano, "Terahertz line-of-sight mimo communication: Theory and practical challenges," *IEEE Communications Magazine*, vol. 59, no. 3, pp. 104–109, 2021.

[6] N. Maletic, L. Lopacinski, M. Goodarzi, M. Eissa, J. Gutierrez, and E. Grass, "A study of los mimo for short-range sub-thz wireless links," in *Mobile Communication-Technologies and Applications; 25th ITG-Symposium*. VDE, 2021, pp. 1–6.

[7] M. Sawaby, B. Grave, C. Jany, C. Chen, S. Kananian, P. Calascibetta, F. Gianesello, and A. Arbabian, "A fully integrated 32 gbps 2x2 los mimo wireless link with uwb analog processing for point-to-point backhaul applications," in *2020 IEEE Radio Frequency Integrated Circuits Symposium (RFIC)*. IEEE, 2020, pp. 107–110.

[8] C. Castro, R. Elschner, T. Merkle, and C. Schubert, "100 gbit/s terahertz-wireless real-time transmission using a broadband digital-coherent modem," in *2019 IEEE 2nd 5G World Forum (5GWF)*. IEEE, 2019, pp. 399–402.

[9] H. Zhou, X. Su, A. Minoofar, R. Zhang, K. Zou, H. Song, K. Pang, H. Song, N. Hu, Z. Zhao *et al.*, "Utilizing multiplexing of structured thz beams carrying orbital-angular-momentum for high-capacity communications," *Optics Express*, vol. 30, no. 14, pp. 25 418–25 432, 2022.

[10] D. M. Bodet and J. M. Jornet, "Directional antennas for sub-thz and thz mimo systems: bridging the gap between theory and implementation," *IEEE Open Journal of the Communications Society*, 2023.

[11] C. Lin and G. Y. L. Li, "Terahertz communications: An array-of-subarrays solution," *IEEE Communications Magazine*, vol. 54, no. 12, pp. 124–131, 2016.

[12] D. Lee, H. Sasaki, H. Fukumoto, K. Hiraga, and T. Nakagawa, "Orbital angular momentum (oam) multiplexing: An enabler of a new era of wireless communications," *IEICE Transactions on Communications*, vol. 100, no. 7, pp. 1044–1063, 2017.

[13] R. Chen, R. Yao, W.-X. Long, M. Moretti, and J. Li, "Uca-based oam non-orthogonal multi-mode multiplexing," *IEEE Open Journal of Antennas and Propagation*, vol. 2, pp. 181–190, 2021.

[14] V. Petrov, J. M. Jornet, and A. Singh, "Near-field 6g networks: Why mobile terahertz communications must operate in the near field," in *GLOBECOM 2023-2023 IEEE Global Communications Conference*. IEEE, 2023, pp. 3983–3989.

[15] D. Bodet, V. Petrov, S. Petrushkevich, and J. M. Jornet, "Sub-terahertz near field channel measurements and analysis with beamforming and bessel beams," *Scientific Reports*, vol. 14, no. 1, p. 19675, 2024.

[16] C. A. Balanis, *Antenna theory: analysis and design*. John wiley & sons, 2016.

[17] S. Schindler and H. Mellein, "Assessing a MIMO channel," *Rohde & Schwarz white paper, Tech. Rep*, 2011.

[18] J. G. Proakis and M. Salehi, *Digital communications*. McGraw-hill, 2008.

[19] H. Abdellatif, V. Ariyarathna, S. Petrushkevich, A. Madanayake, and J. M. Jornet, "A real-time ultra-broadband software-defined radio platform for terahertz communications," in *IEEE INFOCOM 2022-IEEE Conference on Computer Communications Workshops (INFOCOM WKSHPS)*. IEEE, 2022, pp. 1–2.

[20] S. Abu-Surra, W. Choi, S. Choi, E. Seok, D. Kim, N. Sharma, S. Advani, V. Loseu, K. Bae, I. Na *et al.*, "End-to-end 140 ghz wireless link demonstration with fully-digital beamformed system," in *2021 IEEE International Conference on Communications Workshops (ICC Workshops)*. IEEE, 2021, pp. 1–6.